
Review of Observations from the Far Infrared to Radio Wavelengths of the AGB Mass Loss

Arancha Castro-Carrizo

Institut de RadioAstronomie Millimétrique, 300 rue de la Piscine, 38406 Saint Martin d'Hères, France ccarrizo@iram.fr

Summary. This is a review of the most relevant results obtained since the previous *Asymmetrical Planetary Nebula* meeting, in July 2003, providing information on the presence of asymmetries in the circumstellar envelopes of AGB stars, from the far infrared to radio wavelengths. The AGB mass loss is known to be mostly isotropic and the mass loss rate approximately constant (in time scales of about a few thousands years). More and more maps of radio lines show, however, anisotropies and temporal variations in the mass loss of AGB stars. Some few AGB circumstellar envelopes present axisymmetric mass distributions similar to those usually found around post-AGB stars.

1 Introduction

At the time of the last *Asymmetrical Planetary Nebula* meeting, in July 2003, the AGB mass loss was thought to be mostly isotropic and constant in a few 1000 yr. However, some anisotropies and time variations had been already observed in some few objects. The optical image obtained by Mauron & Huggins [21] showed, in light scattered by dust grains, rings and arcs within the extended circumstellar envelope (CSE) around the AGB star IRC+10216. Similar arcs or rings were not seen around any other AGB star before 2003, but they were found in the optical images of several PN and young PN (see [30] and references therein).

Observations of maser emission of OH, H₂O and mainly SiO have provided information about the presence of structure in the innermost layers of many CSEs from the operation of the large networks of VLBI, in the Nineties. Maser emission is found to be concentrated in spots close to the star, in spatial scales of tens of milliarseconds, within a few stellar radii of the stellar surface, between the hot molecular inner envelope and the cooler region at 3-5 stellar radius, where the dust forms. Incomplete clumpy shells are observed in SiO, predominantly in expansion, and with some other complex motions (see e.g. [6]).

In the Far Infrared, IRAS provided data in a large sample of AGB stars (see e.g. [35], [14] and [34]). The spatial resolutions of such maps ($\sim 1'$ at $60\mu\text{m}$) did not allow however an analysis of the presence of asymmetries. ISO/ISOPHOT provided higher spatial resolution, $\sim 20''$ at $90\mu\text{m}$, and some structure was detected in CSEs.

For instance, Izumiura et al. [17] noticed that in Y CVn the star is not located at the center of the extended emission and that the brightness is not constant around the shell. A variation in the mass loss rate in a time scale of ~ 10000 yr was also deduced.

CO is thought to be the main tracer of mass around AGB stars. Most of what we knew in 2003 about the mass distribution around AGB stars came from the wide atlas of CO emission by Neri et al. [24]. They observed between 1992 and 1995 with the Plateau de Bure (PdB) interferometer a large sample of AGB stars. This work was important to determine the averaged characteristics of the AGB circumstellar envelopes (sizes, masses, temperatures), and allowed the confirmation that the AGB mass loss is roughly isotropic. They missed however spatial resolution and sensitivity to study more in detail the characteristics in the mass loss.

From then until 2003 only a few peculiar AGB circumstellar envelopes were mapped in molecular lines. TT Cyg and U Cam were observed by [25] and [19], respectively, and around both stars a large, detached, thin shell surrounding a second, compact mass loss was found. Note, however, that the presence of detached shells as those seen in U Cam and TT Cyg are thought to be a peculiarity of the mass loss of a few AGB stars. Otherwise, only the CSE around IRC +10216 had been well mapped with an interferometer. Fong et al. [8] mapped the $^{12}\text{CO } J=1-0$ emission by combining BIMA millimeter array and NRAO 12m telescope observations. They obtained a spherical large envelope, of $\sim 250''$ in diameter, with multiple brighter clumpy arcs, incomplete shells, expanding at a constant velocity. They proved therefore the presence of mass loss fluctuations at short time scales, of ~ 1000 yr, confirming the nature of those structures seen in the optical [21] or by mapping other molecular lines [13].

Continuum emission at 1mm was also imaged in IRC +10216 by [12], but the spatial resolution of $11''$ did not allow a conclusion about the presence of asymmetries in the mass loss.

In the next sections, a review of the observations providing information about the presence of asymmetries in AGB CSEs, since July 2003, is presented. Many important results were obtained in the last years due to operation of instruments with higher and higher spatial resolution and sensitivity, and also the improvement of the analysis techniques.

2 Far Infrared Imaging

MIRIAD is a project aiming to trace the mass-loss history of large AGB envelopes by imaging the FIR emission (at $70\mu\text{m}$ and $160\mu\text{m}$) using MIPS at the Spitzer Space Telescope. Ueta et al. [32] presented the first MIRIAD results for the AGB star R Hya. The $70\mu\text{m}$ map (Figure 2) shows an arc-like surface brightness distribution surrounded by fainter emission of $\sim 400''$ in diameter. This parabolic distribution is interpreted to correspond to shock-excited line emission (such as [O I] $63\mu\text{m}$ and $146\mu\text{m}$) and locally heated dust emission arising from a stellar-wind bow shock interface between the ISM and the swept-up AGB wind of this moving star (see [32]). The asymmetries seen in the CO profiles (e.g. [31]) are likely explained by the presence of the bow shock, inclined with respect to the line of sight. Wareing et al. [33] reproduce, with a three-dimensional hydrodynamic code, the observed large arc-shaped structure and its surroundings in terms of the interaction of the AGB

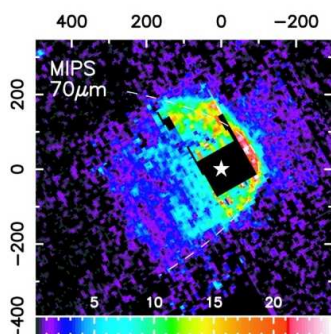


Fig. 1. Background/PRF-subtracted, mosaicked MIPS maps of R Hya at $70\mu\text{m}$. The position of the star is indicated by the star. The tick marks indicate the angular offsets in arcseconds. Linear color scaling of surface brightness (in MJy sr^{-1}) is shown at the bottom. A parabolic curve, which closely represent the stellar-wind bow shock near the apex, is displayed by the dash lines.

wind with the interstellar medium (ISM). They also speculate that the presence of detached shells around other AGB stars may be due to the interaction with ISM.

In addition, in these proceedings Ueta et al. present the program MLHES, which is observing with the AKARI IR satellite the extended dust envelopes around a sample of evolved stars.

3 Mapping Maser emission

Several relevant works were performed in the last years on SiO maser emission in AGB circumstellar envelopes. Cotton et al. ([3] and [4]) monitor the emission of two SiO masers in nine Mira variable stars over several pulsation cycles. The size of the maser rings is found to vary by 3–14% with time, consistent with models [16], but show no clear correlation with the pulsation phase. The lifetime of individual spots is generally shorter than the interval between observations, of three months. The linear polarization fraction is found to show strong variations between epochs. The polarization vectors are mostly tangential to the masing shell, indicating a radial magnetic field. Rotation is possibly detected in Mira. Several jet-like features are seen for Mira and R Aqr at several epochs. In addition, note that the SiO maser shell monitored by [7] in TX Cam shows significant asymmetry and can be best described as a fragmented or irregular ellipsoid at many observational epochs. For VY CMa [26] some maser components seem offset from the inner stellar envelope, may be part of a larger bipolar outflow.

Soria-Ruiz et al. in [27], [28] and [29] analyze the distribution and characteristics of the emission from different masers of ^{28}SiO and ^{29}SiO . The different radial distributions obtained for different ^{28}SiO masers are in contradiction with theoretical predictions. It seems that H_2O IR lines could alter the conditions to produce SiO maser emission.

4 Mapping Molecular Gas

In the last years, there have been several projects aiming to map the molecular line emission in different AGB CSEs. The improvement of the interferometers (including the arrival of the SMA), and also of the techniques to merge interferometric and single-dish data, can explain this increasing interest. CO is thought to be the best

tracer of the mass-loss, and so mapping the emission of low- J CO lines is the aim of most projects.

Interferometers filter out a large amount of the flux emitted by many circumstellar envelopes, which can be recovered by adding visibilities at shorter baselines coming from single-dish observations (see [1]). The techniques to merge single dish and interferometric data have significantly improved.

Lindqvist et al., in preparation, performed On-The-Fly (OTF) observations with the IRAM 30m telescope of the CO $J=2-1$ emission in U Cam, and merged them to the interferometric data published in [19]. The resulting merged data show (in Figure 2) that there is emission also between the present mass loss and the outer shell detected by [19]. In addition, we can see that the extended, roughly spherical, envelope around U Cam presents asymmetries at large scale (from west to east) and also in the smaller scale structure, with the presence of clumpiness.

Hirano et al. [15] mapped the CO $J=3-2$ and $2-1$ line emission in V Hya with the SMA. The maps show fast, collimated winds expanding perpendicular to a disk-like distribution, which may be the remnant of a previous isotropic wind. Chiu et al. [2] imaged, also with the SMA, the CO $J=2-1$ emission in π^1 Gru. A slowly expanding equatorial wind and a high-velocity bipolar outflow are also identified in the CO distribution of this S star.

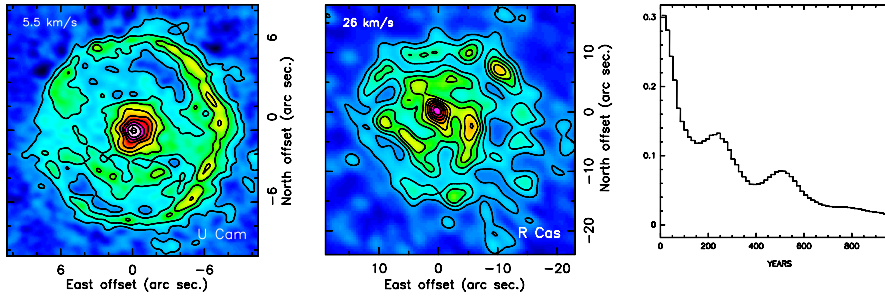


Fig. 2. (*Left:*) $^{12}\text{CO } J=2-1$ emission in U Cam at the systemic velocity, by Lindqvist et al. in preparation. (*Center:*) $^{12}\text{CO } J=1-0$ brightness distribution in R Cas at the systemic velocity, by Castro-Carrizo et al. in preparation. (*Right:*) Azimuthal average of the brightness distribution shown for R Cas, where the distance has been converted to kinematical time.

Some other works imaged the CO distribution in other few AGB stars, e.g. [9], [22] and [23]. Although in some of these maps asymmetries are identified, a deep analysis cannot be made due to insufficient spatial resolution, sensitivity, or to the lack of short-spacing data.

Observations of CO in a large survey of AGB stars are being carried at IRAM with the PdB interferometer and the 30m telescope. We aim at determining the mass-loss history in AGB stars: their geometry, kinematics, photodissociation radius, clumpiness, the ejections of collimated fast winds, etc. A sample of 35 AGB stars has been selected to represent their diversity in the evolutionary status, initial masses, chemical classes, variability types and peculiarities in the CO profiles. In order to study the last phases of the AGB mass loss and the transition to the post-AGB

phase, 10 early post-AGB stars have been added to the sample of AGB stars. The strategy of the program consists in observing with the PdB interferometer two close sources in two tracks, in the so-called *track-sharing* mode. When needed, short-spacing observations are carried out with the 30m telescope, either in the OTF mode, mapping of a few points, or just observing at the central position. Some of the results so far obtained are presented here.

In Figure 2 it is shown the $^{12}\text{CO } J=1-0$ line emission at the systemic velocity in R Cas. Arcs, perhaps incomplete shells, are detected at different radii. Also in Figure 2 we see that the azimuthal brightness average presents variations in a time interval of ~ 250 yr, which can be interpreted in terms of mass loss fluctuations. We also notice some departures from spherical symmetry. If we suppose that the detected arcs come from two concentric shells, they are not spherical. Otherwise, we could speculate whether the arcs belong to a non-spherical distribution, e.g. a spiral.

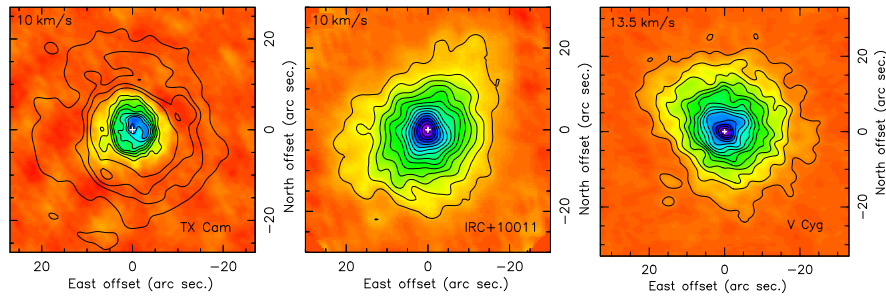


Fig. 3. In the plot on the *left*, the innermost eight contours present the brightest $^{12}\text{CO } J=2-1$ emission in TX Cam, at the systemic velocity. The outermost four contours show a more extended circumstellar component traced by the $^{12}\text{CO } J=1-0$ emission. The $^{12}\text{CO } J=1-0$ line emission is shown, at the systemic velocity, in IRC +10011, at the *center*, and in V Cyg, on the *right*.

The $^{12}\text{CO } J=1-0$ line emission (also $J=2-1$ for TX Cam) at the systemic velocity in TX Cam, IRC +10011 and V Cyg are shown in Figure 3. Although in the three cases the overall circumstellar envelopes are roughly spherical, we distinguish clear asymmetries. TX Cam presents a hook-like structure in the innermost region peaking at the center, where the star is. It is not clear however that the outmost layers of the envelope (seen in CO $J=1-0$) are centered at the same position. For IRC +10011, although the innermost layers of its CSE are quite spherical, the outermost ones show some elongation. Finally in Figure 3, we notice that the brightness peak in the V Cyg map, at the systemic velocity, is not at the center of the circumstellar envelope.

In Figure 4 some channel maps are shown of those obtained with a resampling of 2 km s^{-1} for χ Cyg and RX Boo. The channels displayed for χ Cyg are selected to show changes in the position of the CO emission at different velocities, which interpretation is not clear yet. Departures from symmetry are somehow seen in all channels. For RX Boo we clearly identify a symmetry axis and a position-velocity

gradient, consistently in all channels, which reminds those seen in X Her, V Hya and IRC +50049, in Figure 5.

In Figure 5 we see the position-velocity diagram of the CO $J=1-0$ line emission along the symmetry axis of X Her, and of the CO $J=2-1$ emission along the symmetry axis of V Hya and of IRC +50049. In the three cases we have axisymmetric brightness distributions probably resulting from hour-glass-like structures. V Hya and X Her seem to show some traces of gas expanding along the symmetry axis. A deeper analysis is still needed to determine the kinematic field of those structures.

Results for 9 of the 35 AGB CSEs in the IRAM program are presented here. Departures from spherical symmetry at some degree are found, either at large or small spatial scale, in most of the maps so far observed and spatially well resolved. Particularly, four of them (RX Boo, IRC +50049, V Hya and X Her) present strong axisymmetries, the four sources being peculiar variables. A goal of the program is to relate characteristics of the CSEs to the nature of the stars, their evolutionary status, chemistry, etc. A deep analysis on the presence of asymmetries in the AGB will be carried out as soon as the observational sample is completed. The presence of clumpiness is particularly under investigation. Preliminary results from radiative-transfer modeling of our sample, by Schoier et al. in preparation, indicate that changes of the mass-loss rate in time intervals of \sim a few hundreds years may happen in many AGB stars.

5 21cm HI imaging

Finally, observations of the 21cm HI line emission with the NRT (by [18], [10] and [11]) and with the VLA (by [20]) with beams $\approx 2'$ also suggest the presence of asymmetries in the most extended CSE regions around EP Aqr, X Her, RS Cnc and R Cas.

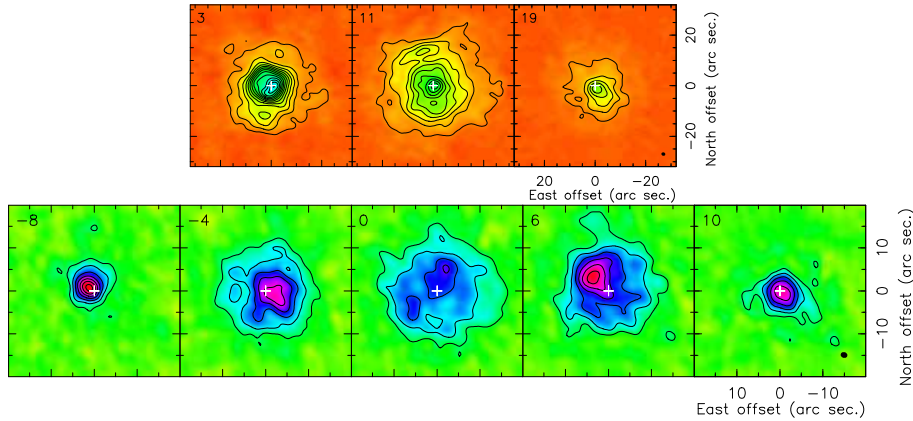


Fig. 4. *Upper*, three channels of the maps of the $^{12}\text{CO } J=1-0$ emission obtained for χ Cyg, with a spectral resampling of 2 km s^{-1} . *Bottom*, five of the channel maps the $^{12}\text{CO } J=1-0$ emission in RX Boo, obtained with a spectral resampling of 2 km s^{-1} .

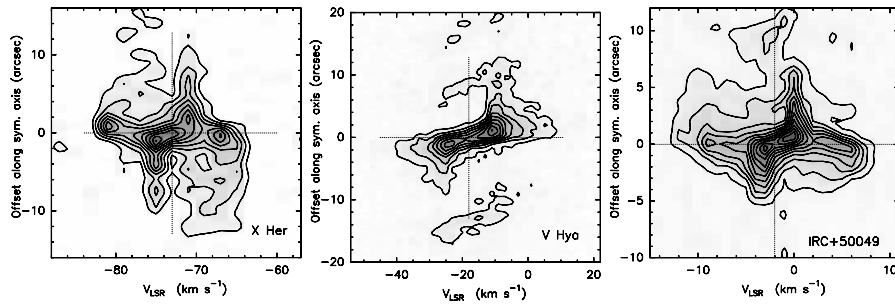


Fig. 5. Position-velocity diagram of the (*left*) CO $J=1-0$ line emission along the symmetry axis of X Her, and of the CO $J=2-1$ brightness distribution along the symmetry axis of (*center*) V Hya and of (*right*) IRC +50049.

References

1. A. Castro-Carrizo, R. Neri, J.M. Winters, et al. In: *Mapping ^{12}CO line emission in CSEs around evolved stars*, ed by F. Kerschbaum, C. Charbonnel, and B. Wing (ASP Conference Series, Vol 378, 2007)
2. P.-J. Chiu, C.-T. Hoang, Dinh-V-Trung, et al.: *ApJ* **645**, 605 (2006)
3. W.D. Cotton, B. Mennesson, P.J. Diamond, et al.: *A&A* **414**, 275 (2004)
4. W.D. Cotton, W. Vlemmings, B. Mennesson, et al.: *A&A* **456**, 339 (2006)
5. S. Dehaes, M.A. Groenewegen, L. Decin et al.: *MNRAS* **377**, 931 (2007)
6. J.F. Desmurs, V. Bujarrabal, F. Colomer, et al.: *A&A* **360**, 189 (2000)
7. P.J. Diamond and A.J. Kemball: *ApJ* **599**, 1372 (2003)
8. D. Fong, M. Meixner, and R. Y. Shah: *ApJ* **582**, L39 (2003)
9. D. Fong, M. Meixner, and E.C. Sutton: *ApJ* **652**, 1626 (2006)
10. E. Gardan, E. Gérard and T. Le Bertre: *MNRAS* **365**, 245 (2006)
11. E. Gérard and T. Le Bertre: *ApJ* **132**, 2566 (2006)
12. M.A.T. Groenewegen, W.E.C.J. van der Veen, B. Lefloch, et al: *A&A* **322**, L21 (1997)
13. M. Guélin, R. Lucas, R. Neri, et al. In: *From Molecular Clouds to Planetary*, ed by Y. C. Minh, and E. F. van Dishoeck (IAU Symposium, Vol 197, 2000) pp 365
14. G.W. Hawkins: *A&A* **229**, L5 (1990)
15. N. Hirano, H. Shinnaga, Dinh-V-Trung, et al.: *ApJ* **616**, L43 (2004)
16. E.M.L. Humphreys, M.D. Gray, J.A. Yates, et al.: *A&A* **386**, 256 (2002)
17. H. Izumiura, O. Hashimoto, K. Kawara, et al.: *A&A* **315**, L221 (1996)
18. T. Le Bertre and E. Gérard: *A&A* **419**, 549 (2004)
19. M. Lindqvist, H. Olofsson, R. Lucas et al.: *A&A* **351**, L1 (1999)
20. L.D. Matthews and M.J. Reid: *ApJ* **133**, 2291 (2007)
21. N. Maunon & P. J. Huggins: *A&A* **349**, 203 (1999)
22. J.-I. Nakashima: *ApJ* **620**, 943 (2005)
23. J.-I. Nakashima: *ApJ* **638**, 1041 (2006)
24. R. Neri, C. Kahane, R. Lucas, et al.: *A&AS* **130**, 1 (1998)
25. H. Olofsson, P. Bergman, R. Lucas, et al.: *A&A* **353**, 583 (2000)
26. H. Shinnaga, J.M. Moran, K.H. Young, et al.: *ApJ* **616**, L47 (2004)
27. R. Soria-Ruiz, J. Alcolea, F. Colomer, et al.: *A&A* **426**, 131 (2004)

28. R. Soria-Ruiz, F. Colomer, J. Alcolea, et al.: A&A **432**, L39 (2005)
29. R. Soria-Ruiz, J. Alcolea, F. Colomer, et al.: A&A **468**, L1 (2007)
30. K.Y.L. Su In: *Asymmetrical Planetary Nebulae III: Winds, Structure and the Thunderbird*, ed by M. Meixner, J. H. Kastner, B. Balick, and N. Soker (ASP Conference Proceedings, Vol 313, 2004) pp 247
31. D. Teyssier, R. Hernández, V. Bujarrabal, et al.: A&A **450**, 167 (2006)
32. T. Ueta, A.K. Speck, R.E. Stencel, et al.: ApJ **648**, L39 (2006)
33. C.J. Wareing, A.A. Zijlstra, A.K. Speck, et al.: MNRAS **372**, L63 (2006)
34. L.B.F.M. Waters, C. Loup, K.J.M. Kester, et al.: A&A **281**, L1 (1994)
35. K. Young, T.G. Phillips, and R. Knapp: ApJ **409**, 725 (1993)